Contrib. Plasma Phys. **50**, No. 3-4, 299 – 305 (2010) / **DOI** 10.1002/ctpp.201010049

Multi-Fluid Modeling of Low-Recycling Divertor Regimes

R. D. Smirnov[*1], **A. Yu. Pigarov**[1], **S. I. Krasheninnikov**[1], **T. D. Rognlien**[2], **V. A. Soukhanovskii**[2], **M. E. Rensink**[2], **R. Maingi**[3], **C. H. Skinner**[4], **D. P. Stotler**[4], **R. E. Bell**[4], and **H. W. Kugel**[4]

[1] University of California San Diego, La Jolla, CA 92093, USA
[2] Lawrence Livermore National Laboratory, Livermore, CA 94551, USA
[3] Oak-Ridge National Laboratory, Oak Ridge, TN 37831, USA
[4] Princeton Plasma Physics Laboratory, Princeton, NJ 08543, USA

Received 02 September 2009, revised 08 November 2009, accepted 05 January 2010
Published online 10 May 2010

Key words Edge plasma transport, divertor, recycling, UEDGE, liquid lithium.

The low-recycling regimes of divertor operation in a single-null NSTX magnetic configuration are studied using computer simulations with the edge plasma transport code UEDGE. The edge plasma transport properties pertinent to the low-recycling regimes are demonstrated. These include the flux-limited character of the parallel heat transport and the high plasma temperatures with the flattened profiles in the scrape-off-layer. It is shown that to maintain the balance of particle fluxes at the core interface the deuterium gas puffing rate should increase as the divertor recycling coefficient decreases. The radial profiles of the heat load to the outer divertor plate, the upstream radial plasma profiles, and the effects of the cross-field plasma transport in the low-recycling regimes are discussed. It is also shown that recycling of lithium impurities evaporating from the divertor plate at high surface temperatures can reverse the low-recycling divertor operational regime to the high-recycling one and may cause thermal instability of the divertor plate.

1 Introduction

Recently, there has been a growing interest to the low-recycling regime of tokamak divertor operation. This operational regime is expected to occur in the case when lithium, which can efficiently retain hydrogen, is used as the recirculating liquid material or as the recoverable coating on the plasma facing components (PFCs). In the proposed low recycling divertor concept [1], the strongly-absorbing liquid PFCs allow efficient handling of the frequent transient high heat power loads (e.g. type-I ELMs) as well as controlling of the hydrogen plasma density. The low-recycling regimes of the divertor operation can also improve the core plasma performance [1]; the reduction in the core plasma temperature gradients and the increase in the energy confinement time and thus fusion power density are expected. This concept is being studied experimentally on various tokamaks including NSTX experiments with lithium coated divertor [2] and planned Liquid Lithium Divertor Module (see [3, 4] for setup and initial modeling). However, the lack of experiments on current tokamaks with large PFC areas covered with liquid lithium motivates our simulation studies of edge plasma behavior in such regimes.

2 UEDGE model

In the paper, the modeling of recycling regimes of divertor operation is done for the NSTX tokamak, which at present operates with the divertor plates coated with lithium. Recent experiments have shown that the increased deuterium gas puffing is needed for discharges with lithium coatings in order to maintain the high density level of core plasma [2]. In the modeling, we use the 2-dimensional multi-fluid multi-species edge-plasma transport code UEDGE [5]. The code solves the fluid transport equations for plasma and impurity ions together with the simplified set of Navier-Stokes and diffusive transport equations for hydrogen and impurity neutral atoms, correspondingly [5]. The flux-limiter approach is used for parallel plasma momentum and heat fluxes in order to describe the low-collisional transport conditions in the scrape-off layer (SOL) [6]. The flux-limit coefficients

* Corresponding author: e-mail: rsmirnov@ucsd.edu, Phone: +01 858 822 5371, Fax: +01 858 534 7716

are set equal 0.25 and 1.00 for the free-streaming electron/ion heat fluxes and the ion viscosity, respectively. The cross-field plasma transport is described by specifying the 2D profiles of transport coefficients in the diffusive-convective model [7]. The effects of classical plasma drifts are turned off in all the calculations. The transport of all charge states of deuterium, lithium and carbon is simulated simultaneously.

For simplicity, we consider the lower single-null magnetic configuration of NSTX, viz. discharge 119033 at 400ms. The 2D non-orthogonal poloidal computational mesh is used corresponding to the MHD equilibrium within $0.640 \leq \psi_{\rm norm} \leq 1.071$ magnetic flux surfaces, where $\psi_{\rm norm}$ is the normalized magnetic flux being unity at the separatrix. The simulated boundary conditions assume the fixed plasma density at the core interface, n_0, and the gradient length approximation at the wall and private flux region boundaries (see [6]). The Bohm condition for the parallel plasma flow is assumed at the divertor plates. The input parameters correspond to a typical L-mode discharge in NSTX. The core heating power is set at 3MW and the core plasma density is $n_0 = 5.1 \times 10^{13}{\rm cm}^{-3}$. The deuterium gas source equivalent to 500-1000A of ionized atoms is distributed along the wall in the inner-upper quadrant. The wall albedo for deuterium is in the range 0.90-0.99 that implies relatively low wall pumping efficiency.

At present, the model for deuterium retention in lithium is in its infancy. Deuterium retention depends strongly on lithium module design, tokamak conditions, discharge characteristics, power loading history. Here, the ability of lithium coated divertor plates to "pump out" deuterium ions and neutrals is simulated by the recycling coefficient R varying from 1 (no pumping) to 0 (100% pumping) for the both plates. This allows us to explore trends taking place during transition from high- to low-recycling divertor regimes in parametric way.

The lithium and carbon impurities originate from the wall and the plates due to sputtering by ions and neutrals as well as due to thermal evaporation. We assume that lithium coating layer is polluted by eroded carbon with [C]/[Li]=1/4, so carbon is also released as lithium evaporates. We assume 50% probability of sticking of the impurity ions and atoms to the material surfaces. The simulation model includes as electron collisions with other plasma particles (ionization, excitation, and recombination) as well as heavy particle collisions (charge exchange, momentum transfer).

The surface temperature of the divertor plates is not yet calculated self-consistently with the heat power load to the plates. Instead, we perform parametric study of effects of the surface temperature on the plasma (via surface material vapor). The lithium coating evaporation rate is calculated according to Hertz-Knudsen formula and the temperature dependent lithium saturated vapor pressure taken from [8]. The prescribed profiles of the surface temperature across the divertor plates have Gaussian shapes peaked near the strike points. The peak temperature $T_{\rm plate}$ is varied in the range from $500{\rm K}$ to $\sim 900{\rm K}$.

We use ballooning-like profile of cross-field diffusivities and convective velocities for the plasma and impurity species assuming the strong inner/outer (1/4) flux asymmetry [7]. We perform three sets of UEDGE calculations, which differ in the cross-field transport coefficients (low, medium, and high). In the medium transport set, the convective velocity of main ion species monotonically increases radially along the outer mid-plane from -7m/s at the core interface to 20m/s at the separatrix and to 100m/s at the wall [7]. In the low and the high transport sets, the edge transport coefficients are correspondingly 5 times lower and higher with respect to the medium set. When not mentioned directly, the transport coefficients correspond to the medium transport set. Steady state UEDGE solutions are obtained and analyzed below.

3 Transition from high- to low-recycling regime

To explore the effects of the reduced divertor recycling via "lithium pumping" on the edge plasma performance in the simulated NSTX configuration, a set of UEDGE runs are performed with the recycling coefficient R of the divertor plates varying from 0.90 to 0.70 while other model parameters are fixed. However, in this series it is not always possible to get a converged solution with UEDGE for any combination of the recycling coefficient and the deuterium gas puffing rate. Figure 1 displays the plasma ion flux to the outer divertor plate as function of the recycling coefficient for different values of the gas puffing rate, J_0. The obtained UEDGE solutions are indicated by the solid marks corresponding to the different puffing rates: 500A (squares), 750A (circles), and 1000A (triangles). As seen, for a given value of J_0, the ion flux to the plate reduces as the recycling coefficient decreases due to increasing deuterium pumping at the divertor plates. Besides the reduced ion flux, the change in divertor pumping efficiency (via R) also causes an imbalance, $\Gamma_{\rm in} - \Gamma_{\rm out}$, of the integral deuterium particle

fluxes to ($\Gamma_{\rm in}$) and from ($\Gamma_{\rm out}$) the closed magnetic flux surface corresponding to the core plasma interface. For the high values of R, the simulated flux $\Gamma_{\rm in}$ of deuterium neutral atoms into the core exceeds the flux $\Gamma_{\rm out}$ of deuterium ions leaking from the core. At the low recycling values, the particle imbalance is reversed, $\Gamma_{\rm in} < \Gamma_{\rm out}$. Since the transport coefficients are fixed in the analyzed set of runs, for each gas puffing rate there is a UEDGE solution corresponding to the core particle flux balance, $\Gamma_{\rm in} = \Gamma_{\rm out}$, at a given J_0. The flux balance solutions are indicated by the solid curve in Fig. 1. The solutions above the curve correspond to the net particle flux into the core, i.e. there is insufficient pumping to maintain discharge in steady state. The solutions below the curve correspond to the net core particle out-flux, i.e. there is excessive pumping.

The UEDGE solutions with core flux imbalance exist due to the fixed core density boundary condition, and in a real discharge they can be approximately realized only for a limited time while the accumulation/depletion of particles in the core does not change the core density significantly. The ion particle flux $\Gamma_{\rm out}$ depends on the core plasma transport, whereas the neutral flux $\Gamma_{\rm in}$ depends on the transport in the edge plasma. To evaluate the characteristic variation time of the plasma density profiles in the edge, SOL, and the divertor regions we perform additional UEDGE runs. In these runs, we solve the transport equations only for the deuterium particle fluxes (in the medium transport case) and analyzed the spatio-temporal evolution of the plasma density profiles in response to 50% and 25% decrease of the core plasma density versus the stationary profiles obtained with $n_0 = 5.1 \times 10^{13}{\rm cm}^{-3}$. We find that the characteristic time $\tau_{\rm edge}$ necessary to attain the steady state profiles in the edge plasma for the reduced core plasma densities is relatively short 20ms (note, that for impurities and plasma temperature this time is much longer).

In NSTX L-mode discharges, the deuterium inventory in the core plasma ($n_0 V_{\rm core} \sim 2 \times 10^{20}$particles, where $V_{\rm core}$ is the core plasma volume) typically increases during the discharge. At 300-500ms, the net flux into the core at $\psi_{\rm norm} \sim 0.6$ magnetic flux surface is estimated at 10-20A level, which corresponds to the net core flux $\Gamma_{\rm net} = \Gamma_{\rm in} + \Gamma_{\rm NBI} - \Gamma_{\rm out}$, where $\Gamma_{\rm NBI}$ is the particle input due to neutral beam injection (NBI), with $\Gamma_{\rm NBI} \sim 60$A for 3MW NBI power and $\Gamma_{\rm in} - \Gamma_{\rm out} \sim 40 - 50$A. Thus, the estimated core density variation time $\tau_{\rm core} = n_0 V_{\rm core}/\Gamma_{\rm net} \sim 1{\rm s} \gg \tau_{\rm edge}$, so it is likely that the whole deuterium profile evolves on the time scale given by the surface processes determining the deuterium recycling on the plasma facing components.

Returning to Fig. 1, we highlight an important general trend – the decreasing divertor recycling requires the increasing gas puffing rate to compensate the divertor pumping and to maintain the net core particle flux balance, as also observed in experiment [2]. Figure 1 also demonstrates that the ion flux to the outer divertor plate decreases despite the increasing gas puffing, as the recycling coefficient becomes smaller. However, the ion flux tends to saturate for very low recycling coefficients indicating that the recycling plasma source does not play an important role in such regimes. We see that ion flux to the plate drops by order of magnitude from about 20kA (at $R = 0.99$, $J_0 = 500$A) to about 2kA (at $R = 0.70$, $J_0 = 1000$A) corresponding to the transition from high- to low-recycling regime of the divertor operation.

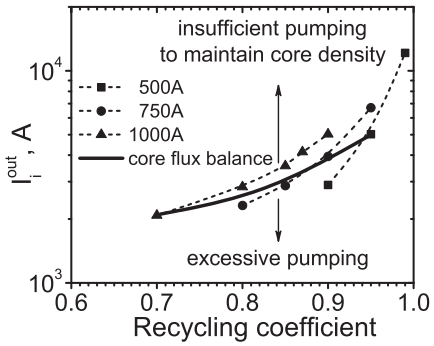

Fig. 1 The plasma ion flux to the outer divertor plate as function of the divertor recycling coefficient for the three different gas puffing rates. The solid curve represents the solutions corresponding to zero net deuterium flux at the core plasma interface. The peak temperature $T_{\rm plate}$ of the divertor plate surface was set to 600K.

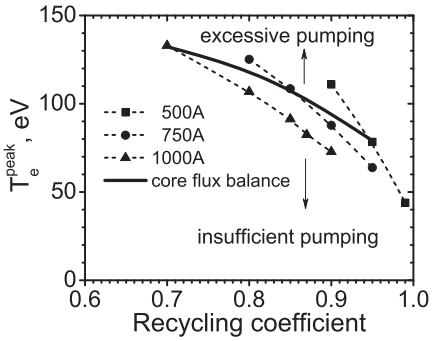

Fig. 2 The peak electron temperature at the outer divertor plate as function of the divertor recycling coefficient for the three different gas puffing rates. The solid curve represents the solutions corresponding to the core flux balance. $T_{\rm plate} = 600$K.

The detailed analysis of the particle balance with UEDGE is a multi-parametric task involving direct matching of experimental plasma profiles. This work is in progress, but it is not the goal of the present paper. Here, we discuss only general trends associated with strong pumping by the material surfaces. Hence, Fig. 1 illustrates in the simple manner the limitations caused by the core particle flux imbalance. Although, the core flux balance curve can shift above or below the simulated one, when we take $\Gamma_{\rm NBI}$ into account, change the core density and/or use a different set of transport coefficients, the major trend appears to be the same.

4 Properties of low-recycling regimes

In Fig. 2 the peak electron temperature at the outer divertor plate as function of the recycling coefficient is shown for the different gas puffing rates. Comparing Fig. 1 and Fig. 2, we see that simultaneously with decrease of the flux to the divertor plate, the peak temperature at the plate corresponding to the core flux balance (solid curve) increases, as the divertor recycling coefficient decreases. Figure 2 shows that the peak electron temperature at the outer plate reaches 100-130eV in the low-recycling regimes compared to 20-50eV in the high-recycling regimes. So, the elevated temperatures are an important feature of the low-recycling regimes.

The high temperatures suggest the transition of the parallel electron heat transport in the SOL from the conduction limited to the convection limited regime. The regime transition is supported by the electron temperature profiles along an open magnetic field line adjacent to the separatrix that are shown in Fig. 3 for the different recycling coefficients and the gas puffing rate of 1000A (the outer midplane position corresponds to 0m). As one can see, the poloidal profiles become almost flat in the low recycling regimes. At the same time, given that the heat flux into SOL changes just slightly, the electron temperature along the magnetic field line significantly increases (Fig. 3), since the parallel particle flux to the plate decreases (Fig. 1), as the recycling coefficient decreases. For electron temperature $T_{\rm e} > 100{\rm eV}$ and plasma density $n_{\rm e} \sim 10^{13}{\rm cm}^{-3}$ characteristic to the simulated low recycling cases, the electron Coulomb collision mean free path exceeds $\sim 15{\rm m}$. This mean free path is comparable with the connection length $\sim 10{\rm m}$ from the outer midplane to the divertor plate that highlights onset of the convection limited regime.

Our simulations also show that in the low recycling regimes the parallel plasma velocity monotonically increases toward the divertor plate reaching the sound speed according to prescribed Bohm boundary condition. Correspondingly, the plasma density drops along the magnetic field line toward the plate, since the plasma particle flux changes weakly in the expanding magnetic flux tube. Such behavior is typical for a free streaming plasma transport regime in the SOL.

Figure 4 compares the radial profiles of the heat load to the outer divertor plate for the low and high recycling coefficients at the same gas puffing rate 1000A. As can be seen, in the low recycling regime the profile becomes narrower in the vicinity of the separatrix due to the faster parallel plasma transport.

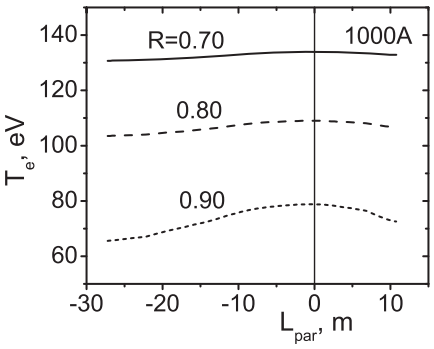

Fig. 3 The electron temperature profiles along a magnetic field line adjacent to the separatrix calculated for the three different values of the divertor recycling coefficient and the gas puffing rate of 1000A. The connection length $L_{\rm par}$ is counted from the outer midplane position.

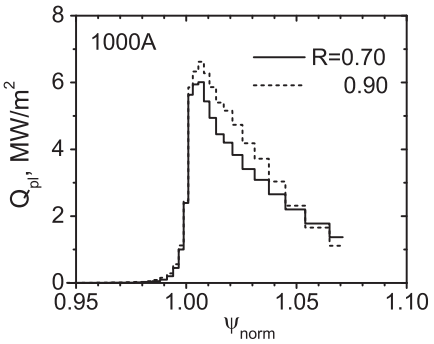

Fig. 4 The radial profiles of the heat flux to the outer divertor plate for the low ($R = 0.70$) and high ($R = 0.90$) recycling coefficients and the gas puffing rate of 1000A. Here, $\psi_{\rm norm}$ is the normalized magnetic flux. Separatrix is at $\psi_{\rm norm} = 1$.

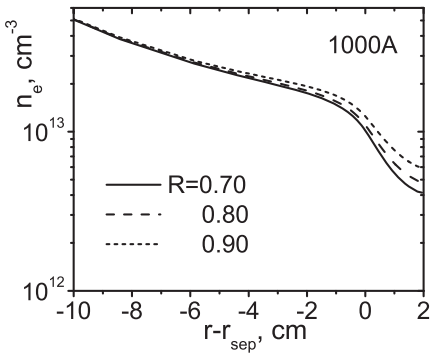

Fig. 5 The radial profiles of the electron density across the outer midplane for the three different recycling coefficients and the gas puffing rate of 1000A. The radial distance $(r - r_{\rm sep})$ is counted from the separatrix position (positive values correspond to SOL).

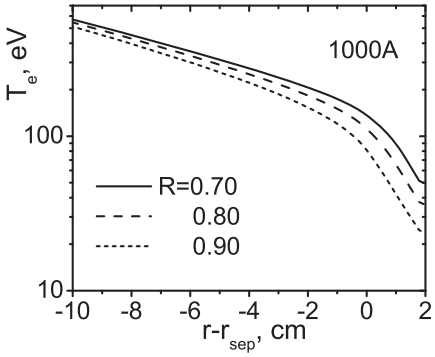

Fig. 6 The radial profiles of the electron temperature across the outer midplane for the three different recycling coefficients and the gas puffing rate of 1000A. The radial distance $(r - r_{\rm sep})$ is counted from the separatrix position.

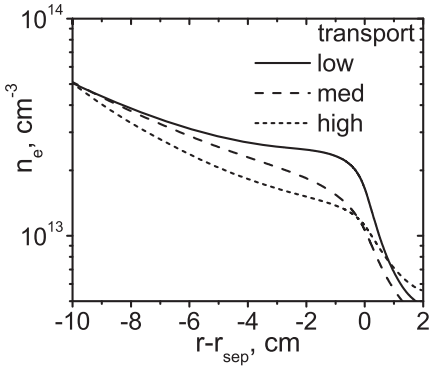

Fig. 7 The radial profiles of the electron density at the outer midplane for the different profiles of the cross-field transport coefficients corresponding to the high, medium, and low radial plasma transport.

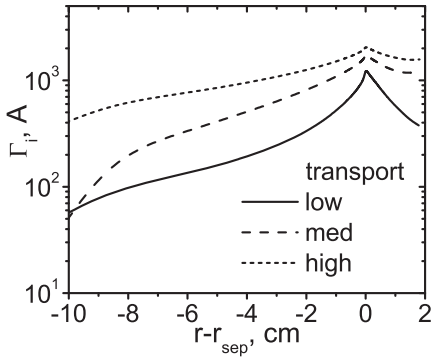

Fig. 8 The radial profiles of the integral cross-filed plasma ion flow in the core edge and SOL for the different profiles of the cross-filed transport coefficients corresponding to the high, medium, and low radial plasma transport.

As the parallel plasma transport in the SOL transits into the free streaming regime, the radial plasma density gradient increases and the density at the separatrix is reduced slightly, reflecting the increased pumping action of the divertor in the case of low recycling (Fig. 5). The higher overall electron temperature increases radial heat conduction coefficients that causes the flatter radial electron temperature profiles (Fig. 6). The decrease of the heat load to the outer divertor plate in the low recycling regime, as shown in Fig. 4, occurs mainly due to redistribution of the heat flux to the inner plate and to the wall.

The role of the radial plasma transport in the SOL to the side wall is demonstrated in Fig. 7 and Fig. 8. Here the radial profiles of the electron density at the outer midplane and of the integral deuterium ion flow through the magnetic flux surfaces in the edge regions (divertor is not included on open flux surfaces) are shown for the three different sets of radial transport coefficients corresponding to the relatively low, medium and high transport. The medium transport case is close to NSTX experimental data [9]. As an expected trend, the density profiles become flatter in the core and the density gradient becomes larger in the SOL due to improved particle confinement, when the radial plasma transport decreases (Fig. 7, low). By contrast, in the high transport case (Fig. 7, high), the density gradient increases in the core and the profile becomes flatter in the SOL.

Figure 8 highlights the important role of particle recycling on the wall. When the cross-field plasma transport coefficients are large (Fig. 8, high, medium), there is significant flux of ions to the wall and the recycled neutrals from the wall, which penetrate deeply into the plasma maintaining the steep plasma density gradients in the core edge. In this case, the integral flux recycling on the wall is about 1kA that is comparable to the gas puffing

rate. By contrast, the reduction of the plasma transport coefficients (Fig. 8, low) substantially decreases the wall recycling, much below the gas puffing rate. In the this case, while the integral radial ion flow in the core and the far SOL regions decreases significantly, the reduction of the flow into SOL through the separatrix is far less substantial. The increase of the electron density at the separatrix by a factor of ~ 2 (Fig. 7) is also relatively small compared to the about 5 fold decrease of the transport coefficients. We explain such behavior by the plasma recycling in the divertor, which continues to supply the recycled neutrals to the SOL that are subsequently ionized in the near-separatrix plasma region, while the recycling at the wall is suppressed.

It is important to note that in the cases when the plasma flux to the wall and the corresponding recycled neutral flux from the wall are substantially reduced (either due to slow radial transport or due to short connection length), the transition from high to low recycling regimes may occur at higher divertor recycling coefficients than those considered here. The requirement for sufficient gas puffing to maintain the core flux balance in the low recycling divertor regimes also may be stronger than simulated in this paper.

5 Impact of divertor plate temperature on plasma parameters and heat load

To explore the influence of the plate surface temperature and lithium evaporation on the divertor operation, we perform a series of UEDGE runs varying the peak temperature $T_{\rm plate}$ in the range 600-900K for the case of 1000A gas puffing rate and the recycling coefficient equal 0.80. The dependence of the peak electron temperature at the outer divertor plate on $T_{\rm plate}$ is plotted in Fig. 9. As can be seen, there is little difference in the electron temperature at the plate for $T_{\rm plate}$ up to ~ 700K due to insignificant lithium evaporation. However, starting from surface temperatures of ~ 800K, the flux of evaporated lithium atoms becomes considerable and leads to marked drop of the electron temperature due to strong lithium recycling and for the temperatures $\widetilde{>}850$K due to impurity radiation energy loss. At the surface temperatures $\widetilde{>}870$K, the flux of recycled lithium ions exceeds the flux of plasma ions to the divertor plate.

Figure 10 displays the peak heat load to the outer divertor as function of the peak surface temperature $T_{\rm plate}$. One can see that the heat load increases by a factor ~ 2, as $T_{\rm plate}$ increases to ~ 850K, due to increasing upstream plasma density and despite the reduced electron temperature. Such behavior may lead to the local surface temperature instability, as the growing heat load causes a further rise of the plate temperature. The mechanism of such instability has been considered by us in detail in [10] using a simplified analytical model. The instability should saturate, when the impurity radiative heat loss becomes significant that leads to decrease of the total heat load to the plate. The formation of a strongly radiative layer and the non-monotonic dependence of the heat load to the lithium limiter on the surface temperatures were observed on T-11M tokamak [11].

The results presented in Fig. 9 and 10 demonstrate that excessive evaporation of the lithium divertor surfaces due to thermally unstable heat load can reverse the low recycling regimes of divertor operation to the high-recycling ones and further to MARFE, when the lithium surface temperature becomes $\widetilde{>}800$K.

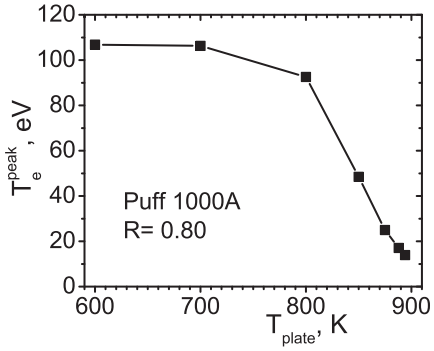

Fig. 9 The peak electron temperature at the outer divertor plate as function of the peak surface temperature of the lithium plate.

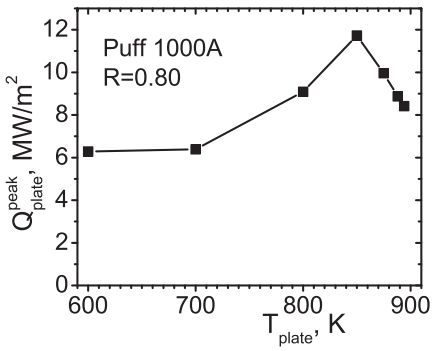

Fig. 10 The peak total heat flux to the outer divertor plate as function of the peak surface temperature.

6 Conclusions

Firstly, we have explored the edge plasma behavior during the transition of the divertor operation from high- to low-recycling regimes using computer simulations with the multi-fluid edge plasma transport code UEDGE for a single-null NSTX magnetic configuration. It has been found that with increasing "lithium pumping", the ion flux to outer divertor plate decreases from 20kA ($R = 0.99$) to 2kA ($R = 0.70$), whereas simultaneously the peak plasma temperature at the plate increases from 20-50eV to 100-130eV. We have also shown that in order to maintain zero net particle flux to the core at the observed core plasma density, the increased hydrogen gas puffing rate is required to offset the increased divertor pumping action in the low-recycling regimes.

Secondly, we studied the properties of low-recycling regime of divertor operation. We have shown that low-recycling regime is characterized by transition of the heat transport in the SOL from the conduction limited to the convection limited regime. This leads to flattening of the parallel profiles and the significant increase of the electron temperature in the edge plasma regions simultaneously with decrease of the plasma particle flux to the divertor plates. It has also been shown that the SOL plasma transport transitions to a free-streaming regime, the radial plasma density gradient increases in the SOL, and the radial profile of the heat load to the outer divertor plate narrows in the low-recycling regimes. At the same time, the upstream radial electron temperature profile becomes flatter due to increased electron heat conduction. It was suggested that suppressing the radial plasma transport in the SOL may lead to establishing of the low-recycling operational regimes at higher divertor recycling coefficients than in the high radial transport cases.

Finally, we have demonstrated that intensive evaporation of lithium surfaces heated above $\sim 800\mathrm{K}$ can reverse the divertor operational regimes from low- to high-recycling. It has also been shown that the heat load to the lithium divertor plate increases due to lithium impurity recycling as the plate surface temperature rises up to $\sim 850\mathrm{K}$ that can lead to the thermal instability of the lithium surface. The further increase of the lithium surface temperature above $\sim 850\mathrm{K}$ has been shown to cause a drop of the heat load to the surface due to the building up radiative energy losses in the divertor, which eventually lead to saturation of the thermal instability.

The obtained results may be helpful for interpretation of recent lithium-coated divertor experiments and future experiments with Liquid Lithium Divertor Module on NSTX as well as for understanding the liquid lithium divertor requirements in the next-step NHTX project. The work on plasma dynamics study via self-consistent modeling of D-Li-C plasma transport and PFC surface temperature is in progress.

Acknowledgements This work was partially supported by US Department of Energy Grant No. DE-FG02-08ER54989 at UCSD and Contracts Nos. DE-AC52-07NA27344 at LLNL and DE-AC02-09CH11466 at PPPL.

References

[1] S. I. Krasheninnikov, L. E. Zakharov, and G. V. Pereverzev, Phys. Plasmas **10**, 1678 (2003).
[2] H. W. Kugel, D. Mansfield, R. Maingi et al., J. Nucl. Mater. **390-391**, 1000 (2009).
[3] J. N. Brooks, J. P. Allain, T. D. Rognlien, and R. Maingi, J. Nucl. Mater. **337-339**, 1053 (2005).
[4] D. P. Stotler, R. Maingi, L. E. Zakharov et al., "Simulations of NSTX with a Liquid Lithium Divertor Module" (this proceedings).
[5] T. D. Rognlien, J. L. Milovich, M. E. Rensink, and G. D. Porter, J. Nucl. Mater. **196-198**, 347 (1992).
[6] T. D. Rognlien, M. E. Rensink, and G. R. Smith, Users manual for the UEDGE Edge-Plasma Transport Code (http://www.osti.gov/energycitations/purl.cover.jsp?purl=/15007243-xnpxNO/native/).
[7] A. Yu. Pigarov, S. I. Krasheninnikov, and B. LaBombard, Contrib. Plasma Physics **46**, 604 (2006).
[8] M. W. Chase Jr. (ed.), NIST-JANAF Thermochemical Tables I, J. Phys. Chem. Ref. Data Monograph **9**, (AIP and ACS for NIST, Washington, D.C. and New York, 1998), pp. 1497,1505.
[9] H. W. Kugel et al., J. Nucl. Mater. **363-365**, 791 (2007).
[10] R. D. Smirnov, S. I. Krasheninnikov, and A. Yu. Pigarov, "On temperature bifurcation of beryllium and lithium plasma facing components in tokamaks" Phys. Plasmas **16**, 122501 (2009).
[11] V. B. Lazarev, E. A. Azizov, A. G. Alekseyev et al. "Quasi-stationary experiment with thin lithium limiter on T-11M", Proceedings of the 30th EPS Conference on Contr. Fusion and Plasma Phys. **27A**, P-3.162 (2003).

